



Structural requirements for the collagenase and elastase activity of cathepsin K and its selective inhibition by an exosite inhibitor

Vidhu Sharma*, Preety Panwar*, Anthony J. O'Donoghue†, Haoran Cui*, Rafael V. C. Guido‡, Charles S. Craik† and Dieter Brömme*

Human cathepsin K (CatK) is a major drug target for the treatment of osteoporosis. Although its collagenase activity is unique, CatK also exerts a potent elastolytic activity that is shared with human cathepsins V and S. Other members of the cysteine cathepsin family, which are structurally similar, do not exhibit significant collagen and elastin degrading activities. This raises the question of the presence of specific structural elements, exosites, that are required for these activities. CatK has two exosites that control its collagenolytic and elastolytic activity. Modifications of exosites 1 and 2 block the elastase activity of CatK, whereas only exosite-1 alterations prevent collagenolysis. Neither exosite affects the catalytic activity, protease stability,

subsite specificity of CatK or the degradation of other biological substrates by this protease. A low-molecular-mass inhibitor that docks into exosite-1 inhibits the elastase and collagenase activity of CatK without interfering with the degradation of other protein substrates. The identification of CatK exosites opens up the prospect of designing highly potent inhibitors that selectively inhibit the degradation of therapeutically relevant substrates by this multifunctional protease.

Key words: cathepsin K, collagen, collagenase, elastase, elastin, exosite.

INTRODUCTION

Cathepsins represent some of the most potent mammalian elastases and collagenases [1,2] and are highly expressed in cell types linked to extracellular matrix (ECM) remodelling [3]. The excessive activity of collagenolytic and elastolytic cathepsins has been associated with bone and cartilage erosion in osteoporosis and arthritis [4,5] as well as with plaque and blood vessel destabilization in atherosclerosis and aneurysms [6,7]. Together, these findings make these cathepsins highly sought-after drug targets [2,8].

Due to its well-known role in bone collagen and vascular elastin degradation, cathepsin K (CatK) is the best-established drug target among cathepsins [9–12]. Most advanced is the understanding of its role in osteoporosis where active site-directed inhibitors have been demonstrated to be effective in phase III clinical trials [13]. However, CatK is a multifunctional protease that also cleaves a wide range of other substrates. CatK has been implicated in the metabolism of regulatory proteins such as the release of thyroid hormones from thyroglobulin [14] and the degradation of tissue growth factor β_1 (TGF- β_1) [15], bradykinin [16] and endorphins [17]. Active site-directed inhibitors targeting CatK will simultaneously block all of these proteolytic functions and thus are likely to cause side effects as alluded to from studies on CatK deficiency [8]. CatK-deficient mice exhibit increased susceptibility to lung fibrosis [18], abnormal airway morphologies [15] and show impairments of their learning and memory capabilities [19]. These CatK deficiency-associated

pathological phenotypes are a concern in the development of active site-directed inhibitors as they have the potential to induce a chemical knockout of CatK during long-term use as expected in osteoporosis treatment. Alternatively, inhibitors that selectively target the ECM-degrading activity but spare the functionality of the active site of CatK are less likely to have side effects. With this objective in mind, we searched for exosites that are selective for the collagen and elastin degradation. Using an analogy model of previously identified exosites in cathepsin V (CatV), we identified two exosites in CatK that are distant from its active site and responsible for the potent collagenase and elastase activity of this protease. Structural modification of these sites by site-directed mutagenesis or the binding of an exosite inhibitor specifically block the collagenase and elastase activity of CatK without interfering with the turnover of non-ECM substrates such as gelatin, thyroglobulin and TGF- β_1 .

EXPERIMENTAL

Construction of exosite variants of CatK and purification

Based on earlier studies of human CatV exosites, putative exosites in CatK were deduced from sequence alignments of human CatK and CatV. The variants were named as exosite mutant 1 (M1), exosite mutant 2 (M2) and combined exosite-1 and -2 mutant 3 (M3). Active enzymes were expressed in methylotrophic yeast *Pichia pastoris* as procathepsins, activated by pepsin, and purified as described in detail in the Supplementary Experimental

^{*}Department of Oral Biological and Medical Sciences, Faculty of Dentistry, University of British Columbia, Vancouver, BC, Canada V6T1Z3

[†]Department of Pharmaceutical Chemistry, Program in Chemistry and Chemical Biology and Graduate Group in Biophysics, University of California at San Francisco, San Francisco, CA 94143. U.S.A.

[‡]Laboratório de Química Medicinal e Computacional, Centro de Inovação em Biodiversidade e Fármacos, Instituto de Física de São Carlos, Universidade de São Paulo, São Carlos-SP 13563-120, Brazil

Abbreviations: CatK, cathepsin K; CatL, cathepsin L; CatS, cathepsin S; CatV, cathepsin V; CBB, Coomassie Brilliant Blue; ECM, extracellular matrix; DHT, p-dihydrotanshinone; GAG, glycosaminoglycan; TFA, trifluoroacetic acid; TGF- β , tissue growth factor β ; WT, wild-type; Z-FR-MCA, carbobenzoxy-phenylalaninyl-argininyl-4-methylcoumarin amide.

To whom correspondence should be addressed (email dbromme@dentistry.ubc.ca).

section. Primers used to create these exosite variants are shown in Supplementary Table S2. The construction of the expression plasmids is described in the Supplementary Experimental section.

Active site titration, enzyme kinetics, stability profile and subsite specificity

Exosite variants were characterized for their kinetic parameters, stability and subsite specificity as described in the supplemental material section.

Elastin degradation assays

Elastin-Congo Red (Sigma-Aldrich) and elastin-rhodamine (EPC Inc.) were used as insoluble elastin substrates at a concentration of 10 mg/ml. They were incubated in assay buffer (100 mM acetate buffer, pH 5.5, containing 2.5 mM DTT and 2.5 mM EDTA) in the presence of 1 μ M wild-type (WT) CatK or its variant cathepsins at 37°C with continuous stirring. Released degradation products in the supernatant were measured using a UV-visible spectrophotometer at 490 nm for elastin-Congo Red and fluorimetrically for rhodamine-labelled elastin (excitation 550 nm and emission 570 nm). The residual elastolytic activities of the enzymes were quantified and normalized against WT CatK. Furthermore, 10 mg/ml unconjugated bovine neck elastin (Sigma–Aldrich) was digested with either 1 μ M of WT or variant CatK in the assay buffer at 37°C, overnight with continuous stirring. The samples were centrifuged and the clear supernatant was loaded on a C18 Altima column (Phenomenex) in water containing 0.1 % trifluroacetic acid (TFA). Fractions were eluted using an increasing gradient of acetonitrile containing 0.1 % TFA. The degradation profile and area under the curve were quantified and analysed using 32 Karat software (Beckman Coulter).

Collagen degradation assays

Bovine type 1 soluble collagen (0.6 mg/ml) (MJS BioLynx Inc.) was incubated in assay buffer (100 mM acetate buffer, pH 5.5, containing 2.5 mM DTT and 2.5 mM EDTA) containing 400 nM CatK or exosite variants in the presence or absence of 400 nM C4-S at 28 °C for 4 h. The reaction was stopped by the addition of 10 μ M E-64 [trans-epoxysuccinyl-L-leucylamido(4-guanidino)butane] and subsequently, the reaction mixture was subjected to SDS/PAGE analysis using 10 % Tris/glycine gels. Bands were visualized by Coomassie Brilliant Blue R-250 (CBB) staining and densitometrically quantified using Image J software (NIH). The collagenase activity was quantified on the basis of the loss of α 1- and α 2-bands after SDS/PAGE. Furthermore, 20 mg/ml of mouse tail fibres were incubated with 2 μ M WT CatK or exosite variants in assay buffer for 18 h. The reaction was stopped using 10 μ M E-64 followed by incubation for 1 h on ice.

SEM of elastin and collagen fibres

SEM was used to characterize elastin and collagen fibres before and after enzymatic treatment as described previously [25,26]. Briefly, 1 mg of bovine neck elastin (Sigma–Aldrich) [20] in 50 μl or 1 mg of mouse tail type I collagen fibres [20] was incubated with 1 μM of WT CatK or exosite variants at 37 °C overnight with shaking. The digested fibres were processed for imaging as described previously [26]. Samples were imaged with a Helios NanoLab^TM 650 (FEI) scanning electron microscope operated at 2–10 kV.

Binding assays

Aliquots of 10 mg/ml of elastin bovine neck or bovine skin type I insoluble collagen (Biobasic Inc.) were separately incubated with either 1 μ M or 0.5 μ M WT CatK or its exosite variants in assay buffer (100 mM acetate buffer, pH 5.5, containing 2.5 mM DTT and 2.5 mM EDTA). The residual activity of unbound enzyme in the supernatant was measured in the aqueous phase at time t = 0and t = 30 min using carbobenzoxy-phenylalaninyl-argininyl-4methylcoumarin amide (Z-FR-MCA) as the substrate. The effect of p-dihydrotanshinone (DHT) to block the binding of CatK on elastin and collagen fibres was determined using E-64 inhibited WT CatK (10 μ M E-64/1 μ M CatK). E-64 inhibited CatK was incubated with either 10 mg/ml of bovine neck elastin (Sigma-Aldrich) or bovine skin collagen fibres (Biobasic Inc.) for 30 min in the absence or presence of increasing concentrations of DHT (12.5–50 μ M). Samples (25 μ l) of the supernatant were separated on 12% polyacrylamide gels by SDS/PAGE and the amount of CatK was determined by densitometry.

Degradation assays for non-ECM substrates

Gelatin (0.6 mg/ml heat-denatured bovine type I collagen) or bovine thyroglobulin (Sigma-Aldrich) (0.6 mg/ml) was treated with 5 nM or 100 nM WT or exosite variants, respectively, in assay buffer (100 mM acetate buffer, pH 5.5, containing 2.5 mM DTT and 2.5 mM EDTA) at pH 5.5 and 28 °C for 4 h. Degradation products were analysed by SDS/PAGE (10 % Tris/glycine gels) and stained with CBB. 40 ng/ml TGF- β_1 (Cedarlane Corp.) was incubated with 50 nM WT or exosite variants in activity buffer, pH 5.5, for 4 h at 28 °C. The reaction was stopped by the addition of 10 μ M E-64. Samples were processed by SDS/PAGE and electroblotted on nitrocellulose membrane. The membrane was blocked with 3% defatted milk (Bio-Rad) and incubated with 1 μ g/ml chicken anti-TGF- β antibody (IgY) (EMD Millipore) at 4°C overnight. The membrane was probed with secondary antichicken antibody (Cedarlane Corp.) 1:1500 in PBST. The bands were visualized using chemiluminescence.

IC_{50} determination for DHT, characterization of its anti-elastase and anti-collagenase activities, and its effect on non-ECM substrates

The IC $_{50}$ values for the anti-elastase and anti-collagenase activities of WT CatK were determined using elastin–Congo Red and soluble collagen degradation assays as described above. DHT was dissolved in DMSO and the assay inhibitor concentrations were between 0.5 and 50 μ M. The DMSO concentration was kept below 1 % (v/v). The effect of DHT (50 μ M) on the degradation of mouse-tail collagen fibres was analysed by SEM as described above. The incubation time was was 18 h for the elastase assays and 4 h for the collagenase assays. Gelatin and thyroglobulin as non-ECM substrates were digested in by WT CatK in the presence of 50 μ M DHT and the reaction was stopped with 10 μ M E-64 after 4 h. The degradation of these substrates was determined by SDS/PAGE analysis as described above. The IC $_{50}$ values for the anti-elastase activity of human CatV and cathepsin S (CatS) were determined as described for CatK.

Molecular docking of DHT to CatK

The 3D structure of the DHT inhibitor was constructed using the standard geometric parameters of the LigPrep utility (version 2.9, Schrödinger, LLC, 2014). Possible protonation states (using Epik, pH 7 ± 2) and potential tautomers were considered during

ligand preparation. OPLS-2005 partial charges were assigned to all of the atoms and subsequently minimized. The resulting structure was exported to the .mol2 format and used in the docking protocol. Molecular modelling was performed using the GLIDE program [21,22] (version 6.2, Schrödinger, LLC, 2014). To execute the docking protocol and to analyse the docking results, the maestro user interface (version 9.7, Schrödinger, LLC, 2014) and PyMOL (version 1.6; Schrödinger, LLC) were employed. The X-ray crystallographic data for CatK determined at 1.7 Å (PDB code 4DMX) [23] was used in the docking simulations. Ligands and water molecules from both structures were removed from the binding pockets. For the docking calculations, hydrogen atoms were added in standard geometry; histidine, glutamine, and asparagine residues in the binding site were manually checked for orientation, protonation and tautomeric states using PyMOL 1.6 side-chain wizard script. GLIDE grid generation wizard was used to define the docking space. Specifically, the binding site was defined incorporating all of the amino acid residues within a radius sphere of 12 Å centred on Cγ of Tyr⁸⁷. Docking was performed using XP (Extra Precision mode) docking protocol [24] and visual inspection was employed to select the representative conformation for the inhibitor.

Statistical analysis

All experiments were performed in duplicate and represented as means \pm S.D. for three independently performed experiments unless otherwise specified. The significance of difference was calculated by one-way ANOVA and P values of ≤ 0.05 were considered significant.

RESULTS

Identification of CatK exosites

Two putative exosites in human CatK were deduced from our earlier observation of surface structures that controlled the elastase activity of CatV [25]. Exosite-1 is located on the outer edge of the L-domain in CatK, which is formed by a hook-like loop spanning from Tyr⁸⁷ to Gly¹⁰² (Figures 1A-1C). This loop structure is conserved in the endopeptidase subfamily of cysteine cathepsins. Out of the 16 amino acid residues forming the loop, eight are conserved in cathepsins K, V, S and L. The loop starts with the conserved tripeptide Tyr^{87} -Pro⁸⁸- Tyr^{89} at the N-terminal loop end, has an acidic dipeptide (Asp/Glu93-Glu94) in its centre, and a conserved Tyr98 and Pro100 at its C-terminal end. Pro88 and Pro¹⁰⁰ are responsible for the upwards direction of the loop, which is stabilized by a disulfide bridge between Cys⁵⁶ and Cys⁹⁶ (Figure 1B). Exosite-2 is located between the L- and R-domain below the S2 subsite pocket where it forms a β -sheet stack with the C-terminal end of the protease (Figure 1B). This exosite is less conserved in its length as well as sequence than exosite-1. Located between conserved residues Gly¹⁰⁹ and Glu¹¹⁸, it is one amino acid longer than the appropriate region in cathepsin L (CatL) and has the same length as in cathepsins V and S (Figure 1A). In contrast to cathepsins K, V and S, CatL has neither significant elastase nor collagenase activity [1,9].

Consequently, we generated three chimera variants of CatK containing corresponding CatL regions and designated them as M1 (exosite-1), M2 (exosite-2) and M3 (combined exosite-1 and -2). These variants were evaluated for their capabilities to degrade elastin, collagen and non-ECM substrates.

Table 1 Enzyme kinetics of WT CatK and its exosite variants

Michaelis—Menten parameters for hydrolysis of Z-FR-MCA by WT CatK and its exosite variants. Values are means \pm S.D. from three independent experiments.

CatK	k _{cat} (s ⁻¹)	K _m (μM)	$k_{\text{cat}}/K_{\text{m}} (\mu \text{M}^{-1}\cdot \text{s}^{-1})$
WT	17.0 + 0.4	9.4 + 1.8	1.80 + 0.4
M1	22.5 + 0.3	$\frac{-}{11.4 + 4.2}$	1.98 + 0.2
M2	25.6 + 0.3	12.8 ± 0.8	1.99 + 0.2
M3	26.0 ± 1.1	14.6 ± 4.0	1.77 ± 0.4
IVIS	20.0 ± 1.1	14.0 ± 4.0	1.77 ± 0.4

Effects of exosite modifications on active site functionality of CatK

To investigate the potential effect of modifications in the exosites on active site functionality, the Michaelis-Menten parameters, k_{cat} and $K_{\rm m}$, the temperature stability of the proteases, and the subsite specificity of the variants were determined. The kinetic parameters showed comparable specificity constants, k_{cat}/K_{m} , towards the substrate, Z-FR-MCA (Table 1) with less than 2-fold variations in their individual k_{cat} and K_{m} values. This indicates that the mutations in these exosites had no overall inhibitory effect. The protease stabilities of WT CatK and its exosite variants also remained mostly unchanged. However, the exosite M2 variant appeared to be slightly less stable than the WT protease and the M1 and M2 variants (Supplementary Figures S1A-S1C). The residual enzymatic activities for WT CatK and its exosite variants decreased overtime at three different incubation temperatures: room temperature, 28 °C and 37 °C. Finally, the effect of exosite modifications on the subsite specificity was investigated. Subsite profiling did not reveal any significant changes in the subsite specificities of S4 to S1 (Figure 1D). The subsite preferences for all protease forms remained the same: S1 prefers Arg; S2 Leu, Ile, and Pro; and subsites S3 and S4 have rather undefined specificities with a slight preference for basic amino acid residues. Together, this indicates that the replacement of exosites in CatK with CatL analogous residues did not significantly alter the overall catalytic efficacy, enzyme stability and subsite specificity in the variants.

Effects of exosite modifications in CatK on the degradation of elastin

Both individual exosite variants, M1 and M2, lost approximately 75-80% of their elastolytic activity towards Congo Red and rhodamine elastin, whereas the activity of the double exosite variant, M3, was reduced by 80–90% when compared with WT CatK (Figure 2A). The same inhibitory effect was demonstrated using bovine neck elastin (Figure 2B). HPLC quantification of degradation fragments revealed more than an 80 % loss of elastase activity in the variant proteases (Figure 2C), which parallels the results seen above. Using a binding assay, it became obvious that the exosites are critical for the binding of the protease to elastin fibres. Almost 90% of WT CatK adsorbed to elastin fibres, whereas the exosite variants remained mostly unbound (Figure 3A). The inhibitory effect of the exosite mutations was also seen by the structural analysis of elastin fibres via SEM. After the digestion of bovine neck elastin by CatK, the smooth fibre surface (Figure 4A, elastin) transformed into loose fibrillar structures (Figure 4B, elastin). In contrast, elastin treated with the variants showed surface morphologies close to that of undigested elastin (Figures 4C–4E, elastin).

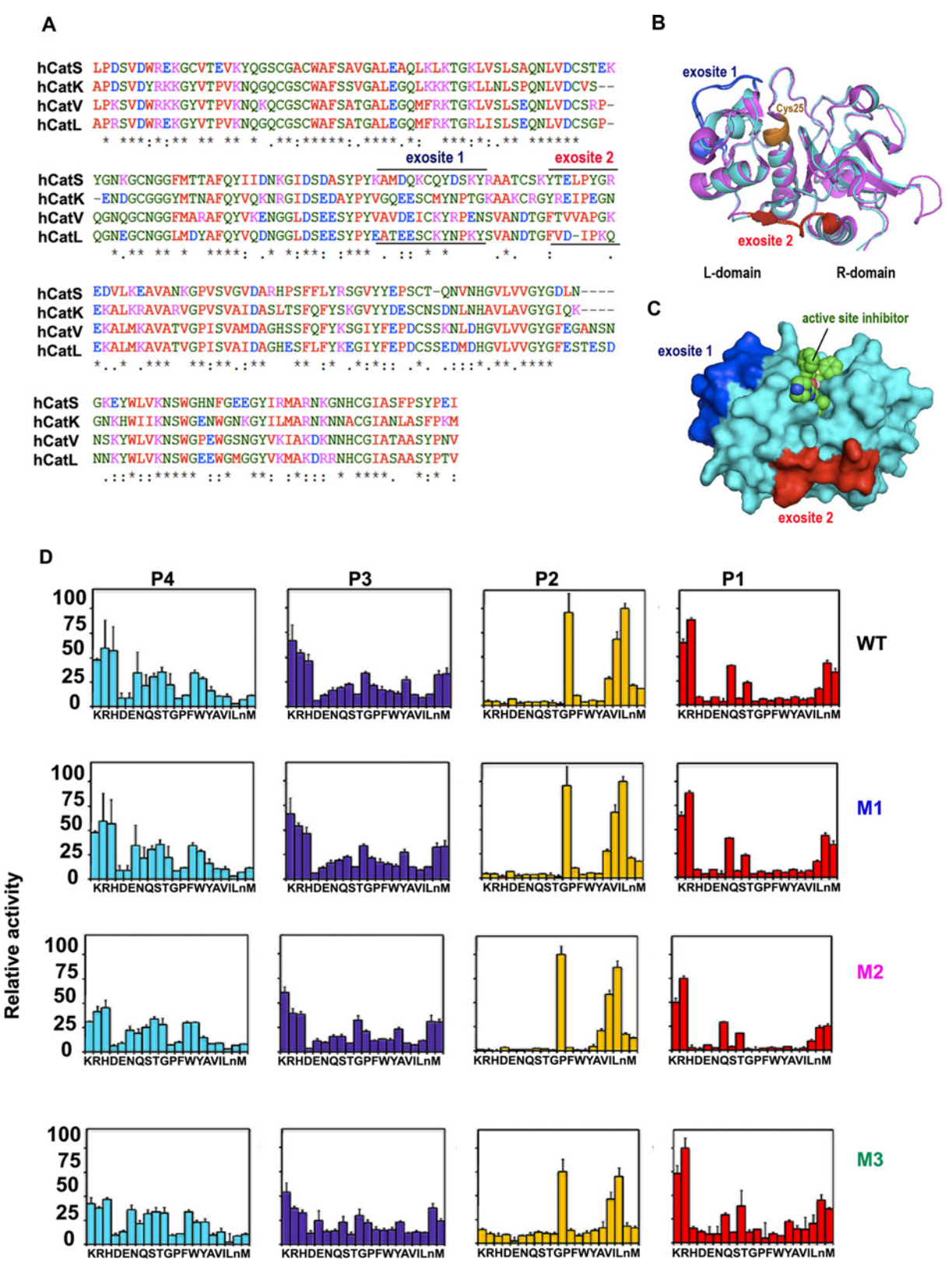


Figure 1 Localization of exosites-1 and -2 on CatK and subsite specificity of CatK and its exosite variants

(A) Sequence alignment of human cathepsins V, L, S and K showing two putative exosite regions using Clustal Ω alignment software. (B) Superimposition of 3D cartoon structures of CatK (cyan) and CatV (purple) reveal highly conserved fold including the putative exosites (exosite-1 in blue and exosite-2 in red). The active site Cys²⁵ residue is shown in orange. (C) Putative exosites in the 3D surface structure of CatK (PDB: 1MEM) are shown in blue (exosite-1) and in red (exosite-2). LHVS, an active site-directed covalent inhibitor, is depicted in green. (D) S4–S1 subsite specificity determination of WT CatK and exosite variants using complete diverse substrate library. P4, P3, P2 and P1 denote the four substrate amino acid residues binding to subsites S4–S1. The *x*-axis indicates a total of 20 amino acid residues. The *y*-axis represents the relative activity of enzyme for each residue referred to the highest activity observed with leucine (L) in the P2 position for WT CatK (= 100). All other activities including those obtained for the variants are calculated as relative activity values to the P2 leucine substrate.

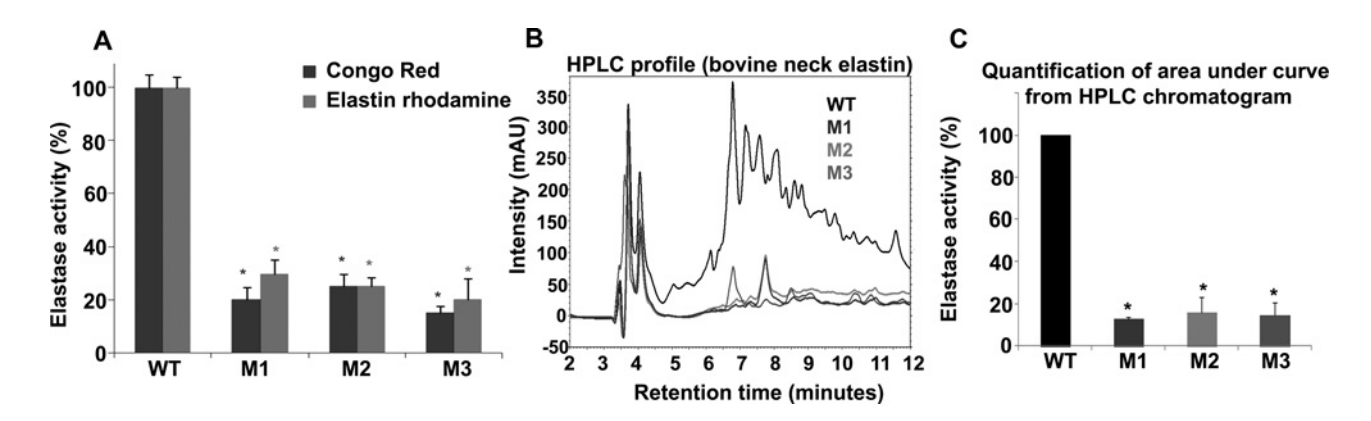


Figure 2 Degradation of fibrous elastin by CatK and its variants

(A) Elastase activity of WT CatK and exosite variants using elastin—Congo Red and elastin—rhodamine substrates. The enzyme concentration was 1 μ M and the substrate concentration was 10 mg/ml. The reaction mix was incubated at 37 °C for 18 h with shaking. The released elastin fragments were spectrophotometrically measured for elastin—Congo Red or fluorimetrically for elastin—rhodamine as described in the Experimental section. The residual activity of each of the mutants was normalized to the WT enzyme (* $P \leq 0.05$). (B) HPLC profile of WT CatK and exosite variant-generated bovine neck elastin degradation fragments. (C) Quantification of bovine neck elastin degradation based on the area under the HPLC chromatogram using 32 Karat software.

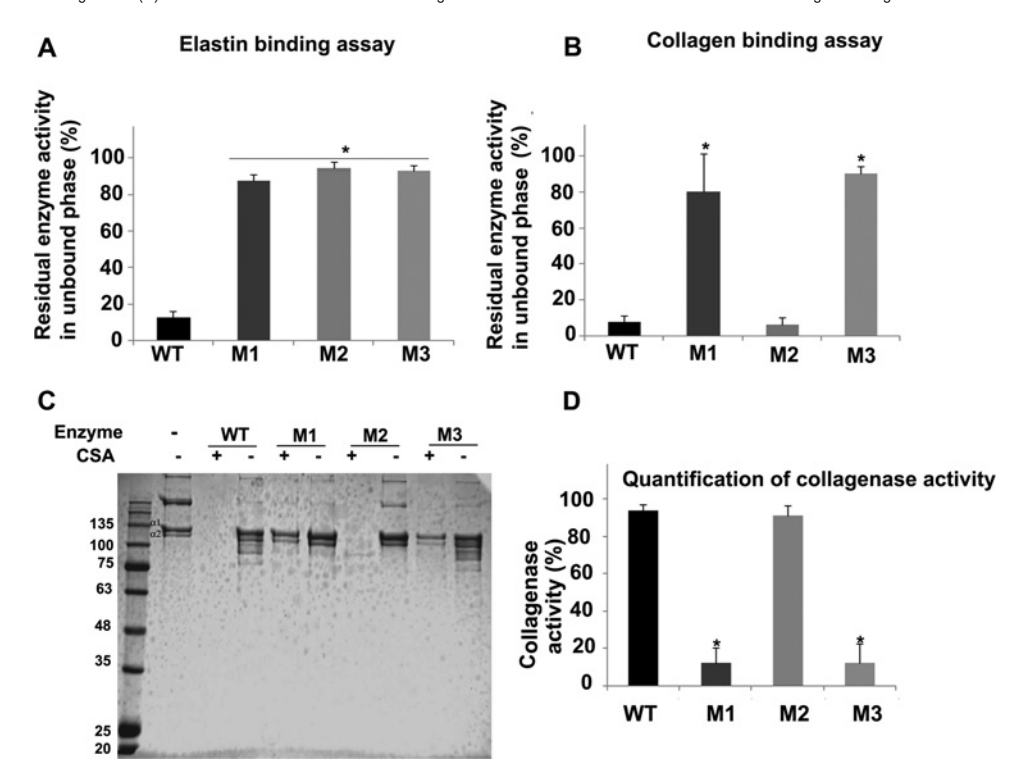


Figure 3 Binding of CatK and its variants to fibrous elastin and collagen and the degradation of collagen

(A) Quantification of the binding of CatK and its exosite variants to fibrillar elastin. (B) Quantification of the binding of CatK and its exosite variants to fibrillar collagen. Results are enzymatic activity as a percentage of unbound protease. Enzyme concentrations were 1 μ M (or 500 nM for collagen binding assay). (C) SDS/PAGE analysis of the collagenase activity of CatK and its exosite variants. Bovine soluble collagen was incubated with 400 nM of enzyme at pH 5.5 and 28 °C for 4 h in the presence or absence of chondroitin 4-sulfate (C4-S). (D) Quantification of collagenase activity is based on the loss of α 1- and α 2-bands using densitometric analysis. Results are means \pm S.D. for three independent experiments (* $P \le 0.05$).

Effects of exosite modifications in CatK on the degradation of collagen

CatK is primarily known as a potent collagenase and therefore the effect of exosite modifications on collagenolysis was investigated. First, we looked into the binding of WT CatK and its variants to collagen fibres. In contrast to elastin binding, only exosite variants M1 and M3 lost their capability to bind to collagen (Figure 3B), indicating that exosite-1 specifically contributes to collagen binding. This suggests a different utilization of exosites

for elastin and collagen hydrolysis. To corroborate the binding results, we next investigated the efficacy of WT CatK and its variants to degrade soluble triple helical collagen and fibrillar type I collagen. The degradation of soluble bovine collagen was inhibited by more than 90% in the M1 variant, whereas the exosite-2 variant, M2, had no effect (Figures 3C and 3D). Furthermore, scanning electron micrographs of WT CatK and variants-treated fibrillar type 1 collagen supported the role of exosite-1 in collagen degradation. The fibre morphology of M1-and M3-treated collagen (Figures 4C and 4E, collagen) was

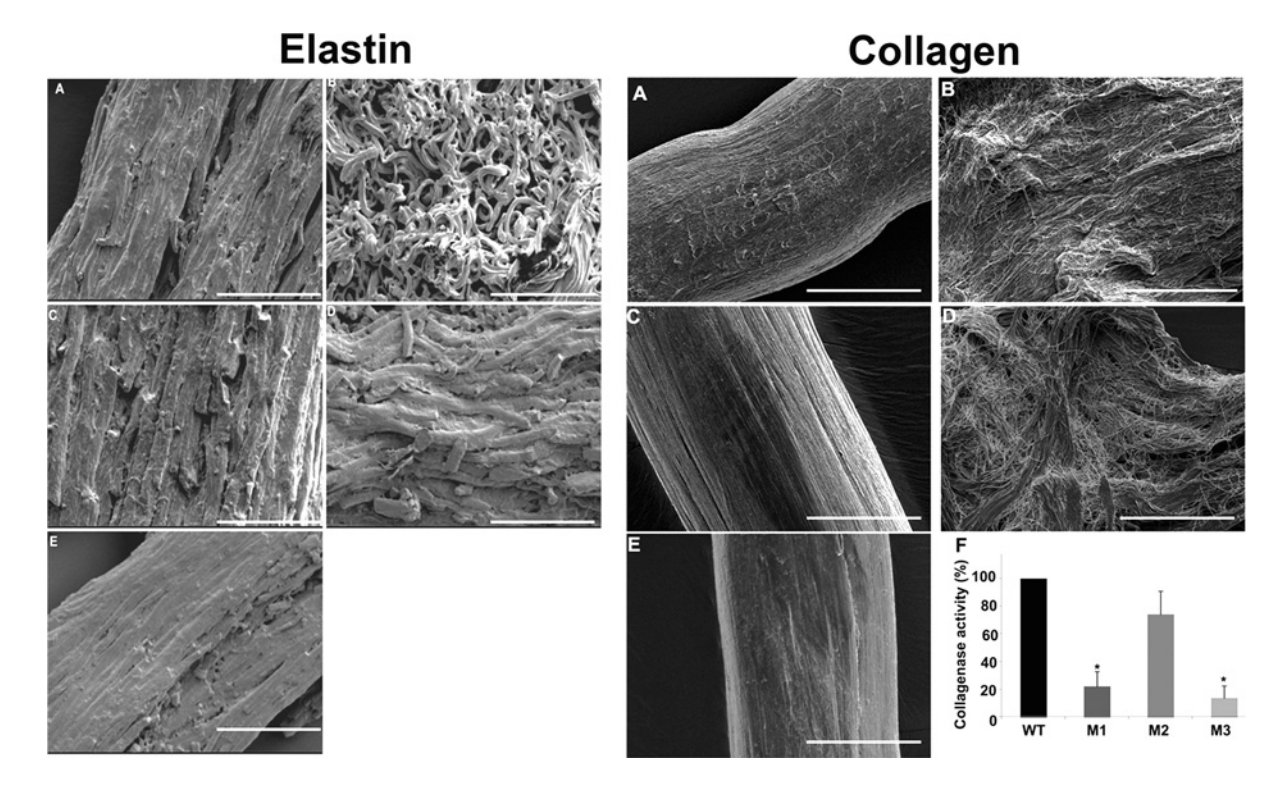


Figure 4 Scanning electron micrographs of bovine neck elastin and insoluble mouse-tail collagen fibres after digestion with CatK or variants

Elastin: (**A**) undigested elastin; (**B**) CatK treated; (**C**) M1 treated; (**D**) M2 treated; and (**E**) M3 treated. Protease concentrations were 1 μ M and the digestions were performed at pH 5.5 and 37 °C for 18 h. Scale bar represents a 50 μ m scale. Collagen: (**A**) undigested bovine skin collagen; (**B**) treated with CatK WT; (**C**) treated with M1 exosite variant; (**D**) treated with M2 exosite variant; and (**E**) M3 variant. Protease concentrations were 2 μ M and the digestions were performed at pH 5.5 and 37 °C for 4 h. Scale bars represent 50 μ m. (**F**) Percentage relative collagenase activity of WT CatK and its exosite variants using insoluble mouse tail fibres based on released soluble collagen fragments (α 1- and α 2-chains). The collagenase activity was quantified by measuring the relative appearance of α -chains released from fibres upon digestion. The quantification was carried out using ImageJ software and results are means \pm S.D. for two independent experiments. Although M1 and M3 showed significant reductions in collagenase activity (*P < 0.05), M2 showed activity comparable with that of CatK.

comparable with that of undigested fibres (Figure 4A, collagen), whereas the action of variant M2 (Figure 4D, collagen) revealed complete collagen fibre disintegration as previously seen for WT CatK [26] (Figure 4B, collagen). The quantitative analysis of fibre degradation in terms of the liberation of tropocollagen fragments from intact fibres is shown in Figure 4F, collagen, which presents the same pattern as revealed in the SEM study. This suggests that only exosite-1 is involved in the degradation of soluble as well as insoluble collagen, whereas exosite-2 appears to be specifically required for elastin degradation.

Effects of exosite modifications on the degradation of non-ECM substrates by CatK

CatK is a multifunctional protease that also hydrolyses a variety of non-matrix proteins. Previous studies identified thyroglobulin [14], $TGF-\beta_1$ [15], aggrecan [27] and endorphins [17] as biologically relevant substrates of CatK. As exosite modifications in CatK did not alter the active site functionality and subsite specificity, the degradability of non-ECM proteins was investigated. First, as a representative generic substrate without a defined structure, gelatin was used. Degradation experiments showed that WT CatK as well as its variants degraded gelatin equally (Supplementary Figure S2A). In addition, the degradability of thyroglobulin and $TGF-\beta_1$ was evaluated. Both substrates were efficiently degraded by WT and exosite variants (Supplementary Figures S2B and S2C). These experiments provided evidence that CatK exosites 1 and 2 are selective for

the degradation of elastin and collagen and do not affect the hydrolysis of other substrates.

Selective inhibition of the collagenase and elastase activity of CatK by an exosite inhibitor

Based on our exosite model, we screened various libraries for anticomplex formation inhibitors of CatK (to be reported elsewhere). Among other compounds, we identified DHT as a potent exosite inhibitor of CatK (Figure 5A). DHT revealed IC50 values of $15 \pm 2 \,\mu\text{M}$ for tropocollagen (Figure 5B) and $11.3 \pm 2.4 \,\mu\text{M}$ for elastin-Congo Red degradation (Figure 5C). The IC₅₀ values represent a 30- and 11-fold molar excess of DHT over CatK in the collagenase and elastase assays, respectively. 25 and 50 μ M DHT completely inhibited the degradation of fibrillar mouse tail collagen and bovine neck elastin, respectively, by CatK (molar 1:25 and 1:50 ratio between CatK and DHT) as shown by SEM (Figure 5D). However, the degradation of non-ECM substrates such as gelatin and thyroglobulin was not blocked in the presence of 50 μ M DHT (5000 and 500 molar excess of DHT over CatK, respectively) (Figure 5E). No inhibition of the hydrolysis of the synthetic substrate, Z-FR-MCA, was observed up to a molar ratio of 1:1000. Binding assays using either fibrous elastin or collagen supported the putative binding of DHT to exosite-1. In the presence of 12.5 μ M DHT, the binding of E-64 inhibited WT CatK to the elastin and collagen fibres was reduced by 70% and 65%, respectively (Figure 5F). Additional increases in the DHT concentration only slightly further reduced the binding to the fibres. DHT also inhibits the elastase activity of human CatV

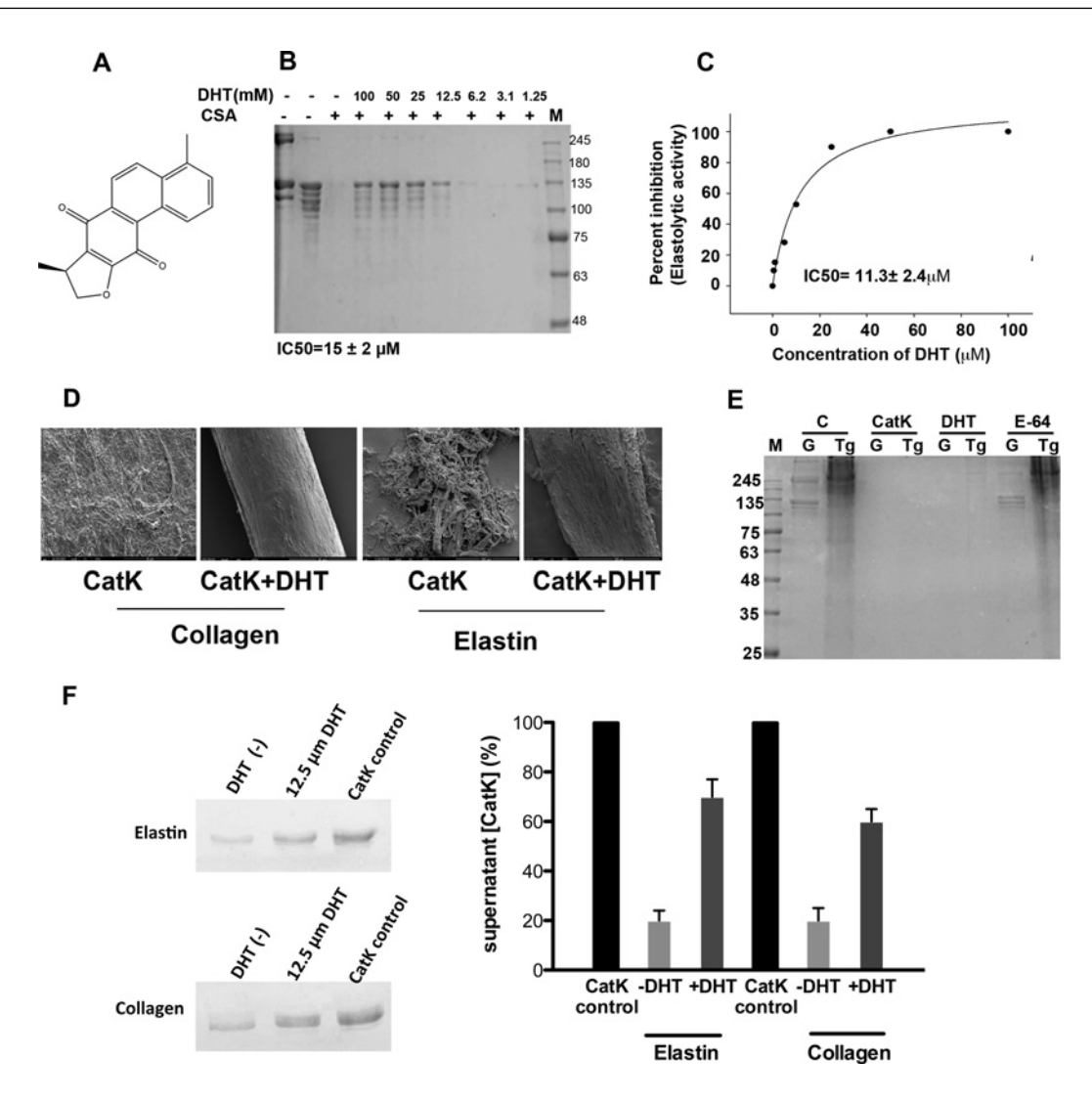


Figure 5 Effect of exosite inhibitor p-dihydrotanshinone (DHT)

(A) Structure of DHT; (B) inhibition of type I soluble collagen by DHT (SDS/PAGE) and (C) IC₅₀ value determination for elastin—Congo Red degradation in the presence of DHT by CatK. (D) SEM images of the inhibition of CatK-mediated mouse tail type I collagen fibres degradation by DHT. (E) Lack of inhibition of CatK-mediated degradation of non-ECM substrates, gelatin and thyroglobulin by DHT (50 μ M) at pH 5.5 and room temperature. CatK is fully inhibited in the presence of 10 μ M E-64. (F) Prevention of elastin and collagen fibre binding to E-64 inhibited WT CatK in the presence of 12.5 μ M DHT.

with an IC₅₀ value of $89 \pm 5~\mu M$, which is approximately 7-fold less efficient when compared with CatK (Supplementary Figure S3). The inhibitory effect of DHT towards human CatS is even less (IC₅₀>100 μM ; less than 40% inhibition at solubility limit of 100 μM of DHT, results not shown).

The calculated best orientation of DHT inhibitor within the CatK exosite is shown in Figures 6(A) and 6(B). The inhibitor establishes polar and hydrophobic contacts with exosite-1 residues. A polar interaction is predicted between the side chain of Asn⁹⁹ and the inhibitor. In our model, the 7-carbonyl substituent of the dihydrophenanthrodione ring is favourably orientated to accept a hydrogen bond from the side-chain ND2 of Asn⁹⁹ (Figure 6C). Additionally, the non-polar parts of DHT make favourable van der Waals contacts with several structural elements of the protein, some of them establishing hydrophobic interactions with the macromolecular counterparts, which significantly contribute to the complex stability. In particular, the 4-methylnaphtyl substituent is docked into the hydrophobic pocket formed by the amino acids Tyr⁸⁷, Pro⁸⁸ and Val⁹⁰, whereas the dihydrophenanthrodione ring is in van der

Waals contacts to the side chain of Met⁹⁷. This putative binding site would explain both the inhibition of the elastase and collagenase activity of CatK and the lack of inhibition of the hydrolysis of the two non-ECM substrates and the small fluorogenic peptide.

DISCUSSION

CatK exploits two exosites for elastin and one for collagen degradation

CatK is the only cysteine cathepsin that has both potent elastase and collagenase activity. Both activities require specific exosite interactions. Although two exosites are needed for the hydrolysis of elastin, only one of them is exploited for collagen degradation. As there were no significant differences observed for the elastolytic activities of variants M1, M2 and M3, each exosite appears to be independent from the others and no additive effect was seen in the double exosite variant. This assumption is supported by binding studies of CatK and its variants to insoluble elastin. The binding assay revealed a strong adsorption of WT

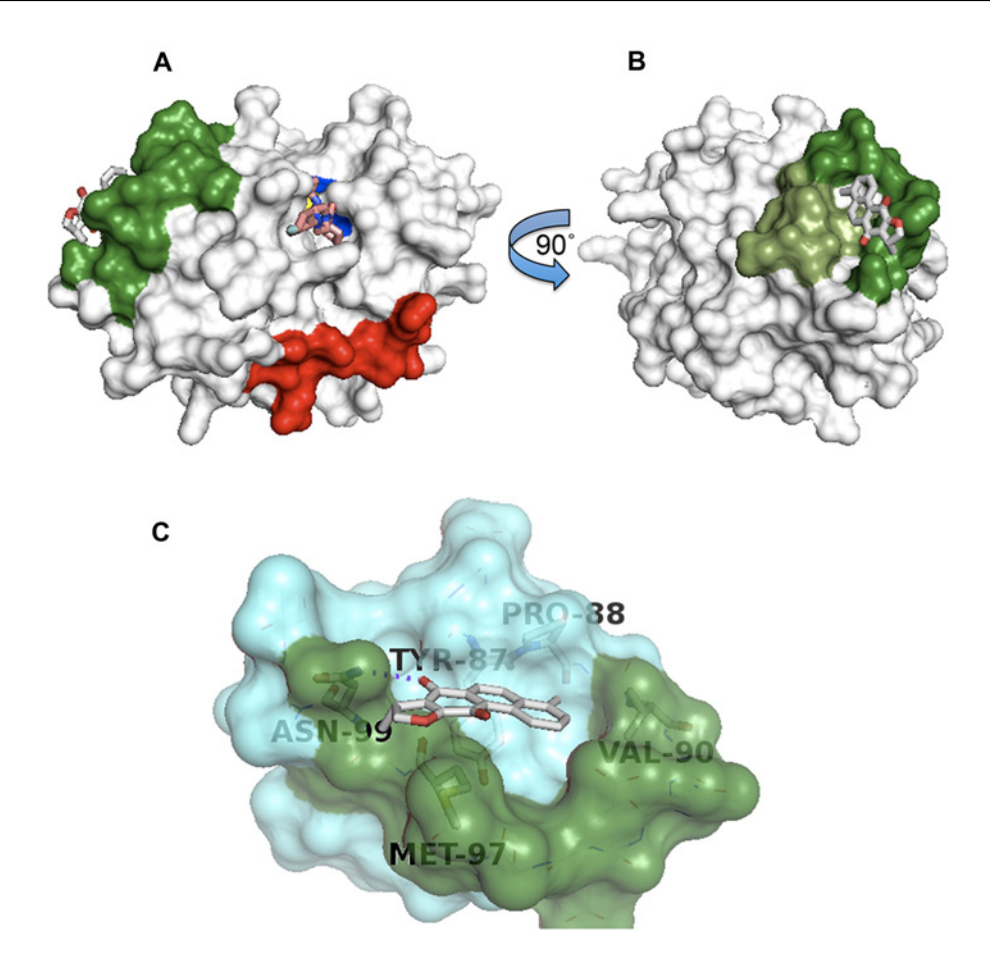


Figure 6 Binding of DHT to CatK

(A) Binding model showing surface view of CatK structure with DHT at exosite-1. Exosite-1 is indicated in dark green and exosite-2 is in red. The catalytic residues Cys²⁵ and His¹⁶² are indicated in yellow and blue respectively. (B) Rotated by 90°. The moss-green shade at exosite-1 shows the boundaries of the DHT-binding site. (C) Predicted binding mode of DHT within CatK exosite-1. DHT is shown as a stick model and the hydrogen bond is shown as a black dashed line. The putative binding mode was determined using the GLIDE program (for experimental details see the Experimental section).

CatK to elastin fibres, whereas the exosite variants remained mostly unbound (Figure 3A). Thus, our exosite model suggests that both exosites on CatK tether the insoluble elastin towards a productive binding mode and guide it to the catalytic site of the enzyme. In contrast, Novinec et al. [28] previously proposed a step-wise binding model where elastolytic cathepsins rapidly adsorb in an initial step to the elastin surface in a non-productive manner, followed by a rearrangement to a catalytically productive complex in which the active centre of the enzyme binds to an elastin peptide. Non-elastolytic CatL would switch rapidly between adsorption and desorption, whereas in our model, it would not bind at all. The adsorption of WT CatK to elastin fibres was between 80 % and 90 %, whereas the exosite variants remained mostly unbound (Figure 3A). Using the GRAVY calculator, we determined that exosite-1 replacement with the analogous CatL region reduced the hydrophobicity score of WT CatK at this site by 65 % (Supplementary Table S2). In general, exosite-1 is significantly more hydrophobic for all three elastolytic cathepsins (CatK, V and S) when compared with CatL. In contrast, the hydrophobicity scores for exosite-2 are very diverse for the four cathepsins with rather hydrophilic values for CatK and L and more hydrophobic values for CatV and S. The common denominator in exosite-2 of CatK and V (and also for CatS) is that in all three elastases this region is one amino acid longer than in CatL (Figure 1A). The deletion of a conserved glycine residue in CatV, which is conserved in the three elastases but not in CatL, reduced the elastolytic activity of the appropriate CatV variant by 30 % [25]. This might reflect a greater influence of the length of the exosite than of its hydrophobicity. As exosite-2 is bridging the L- and R-domain of cathepsins and is located below the substrate specificity defining the S2 subsite, it is likely that this area requires a certain width for accepting a prone elastincleavage site to enter the active site area. The utilization of two exosites might be a general mechanism for elastolytic proteases. Two exosites remote from its active site have also been reported for matrix metalloproteinase-12 [29], which affected the hydrolysis of soluble elastin and to a lesser degree that of insoluble elastin [30]. However, it remains unclear whether the MMP12 exosites are specific for elastin as no other biological protein substrates were analysed.

In contrast to its elastase activity, the collagenase activity of CatK depends on the formation of oligomeric complexes with glycosaminoglycans (GAGs) [31,32]. These CatK complexes are stabilized by distinct GAG binding sites that bridge at least two CatK molecules [32] and by protein–protein interactions within the CatK/GAG complex [33]. Interestingly, the protein–protein interaction site overlaps with exosite-1. X-ray crystallographic studies of CatK/GAG complexes showed head-to-head dimers of CatK via their exosite-1 regions [33]. As exosite-1 is part of the dimer interface site and collagenolytically inactive CatL is

unable to form equivalent complexes in the presence of GAGs [31], it was not surprising that perturbation at the dimer interface led to the observed inhibition of the collagenase activity of CatK. The relevance of exosite-1 for collagenase activity is also supported by an experiment of nature. A Y98C mutation causes the bone-sclerosing disorder pycnodysostosis [34]. Tyr⁹⁸ is located within the exosite-1 loop and is completely conserved in all CatK proteases but absent from other cathepsins. We have previously shown that this mutation completely abrogates the complex formation and thus the collagenase activity of CatK, yet still allows the degradation of gelatin and the synthetic substrate, Z-FR-MCA [35]. This suggests that exosite-1 is not a direct binding site for triple helical collagen but a CatK oligomerization site and that only the CatK complex binds to collagen. In contrast, exosite-2 is distant from the GAG and protein-protein binding sites in the CatK complex and this may explain its irrelevance regarding collagenase activity.

Exosite involvement in collagenases of the matrix metalloproteinase family has been previously discussed and linked to a special non-catalytic domain termed haemopexin [36]. Later studies explored in detail the mechanism of collagen unwinding involving exosites in the haemopexin domain [37–39]. Other than the haemopexin exosites, specific binding sites closer to the active site have also been implicated in the unwinding of triple helical collagen [40]. It should be noted that in the case of CatK, classical subsite interactions are also necessary for the cleavage of collagens as an alteration of the S2 subsite pocket to avert the accommodation of proline prevents collagenolysis [41]. Exosite-1 in CatK is thus neither a remote subsite nor a classical substrate binding exosite but likely a site required for the formation of collagenolytically active CatK oligomers in the presence of glycosaminoglycans.

Exosite inhibitors as selective elastase and collagenase blockers for CatK

Exosite inhibitors or antibodies targeting exosites gained momentum in recent years as they promise increased specificity in drug development [42,43]. CatK is an important drug target for skeletal and vascular diseases [12,44]. To date, numerous active site-directed inhibitors have been generated and evaluated in preclinical and clinical settings [44]. Any active site-directed inhibitor would abrogate the entire proteolytic activity of CatK in addition to the desired blockage of excessive elastin and collagen degradation in these diseases. This is of high relevance as an active site-directed inhibitor, odanacatib, has successfully passed a largepatient number phase III clinical osteoporosis trial [13]. Lack of turnover of substrates such as TGF- β_1 and thyroglobulin as seen in CatK-deficient mice has been associated with adverse effects [15,18,19]. The knowledge of exosites in CatK provides the tools to identify exosite inhibitors that will selectively inhibit its elastase and/or collagenase activity without interfering with the hydrolysis of other physiologically relevant substrates. We identified DHT as a putative exosite-1-targeting inhibitor that selectively blocks the elastase and collagenase activity of CatK with IC₅₀ values in the low micromolar range (11–15 μ M) reflecting a molar enzyme to inhibitor ratio of 1:10-30 in the degradation assays. Neither cleavage of the synthetic peptide substrate, Z-FR-MCA, nor of non-ECM substrates was observed at molar ratios of >1:1000. Although we do not yet have structural proof of the binding of DHT into exosite-1, the significant reduction in WT CatK binding to collagen and elastin by 60 and 75 % in the presence of DHT strongly suggests its binding to exosite-1 (Figure 5F). This corresponds to the 80-90% blocking of the binding of

collagen and elastin fibres to the exosite-1 variant (M1). It is of interest that closely related DHT analogues, which are major constituents in the herb *Salvia miltiorrhiza*, have been recently evaluated for their anti-resorptive activity in cellular and rodent models of osteoporosis [45–48]. *S. miltiorrhiza* is widely used in Chinese traditional medicine for the treatment of osteoporosis [49].

The lack of inhibition of the hydrolysis of the synthetic peptide and two non-ECM substrates by DHT would not support an allosteric mechanism as recently described for a small anthranylic acid derivative (NSC13345). This compound binds on the R-domain and distant from exosite-1 and -2. It blocks the collagenase activity at a concentration of 100–200 μ M and shows a 40–50 % inhibition of the hydrolysis of azocasein and a synthetic peptide substrate at the same, rather high, inhibitor concentration [50]. Furthermore, the lack of any observable changes in the S1–S4 subsite specificities in the exosite variants (Figure 1D) would also contradict an allosteric function of exosite-1 and -2.

Conclusion

We have identified two exosites in CatK that selectively contribute to the hydrolysis of soluble triple helical collagen as well as fibrillar collagen and elastin. Although exosite-1 is required for the degradation of elastin and collagen, exosite-2 specifically contributes to elastin degradation. None of the exosites affect the hydrolysis of non-ECM substrates, suggesting the exclusion of an allosteric effect. This is further supported in that modifications in both exosites do not alter the subsite specificity of protease. We also identified DHT as an exosite-1-targeting inhibitor that selectively blocks the elastase and collagenase activity of CatK without interfering with other proteolytic activities of the protease. Furthermore, DHT reveals some selectivity for the exosite-1 of CatK, whereas the inhibitor effect is at least eight times less with elastolytic cathepsins V and S. This suggests the possibility of further increasing the potency of tanshinone derivatives towards CatK and improving its selectivity. The identification of exosite inhibitors that specifically target the turnover of therapeutically relevant ECM substrates is of high relevance as an active sitedirected inhibitor, odanacatib, is presently evaluated as an antiresorptive drug for the treatment of osteoporosis [13]. Lack of turnover of non-ECM substrates as seen in CatK-deficient mice has been associated with various adverse effects. Therefore, exosites represent novel drug-targeting sites for the substratespecific inhibition of CatK, which can overcome the intrinsic limitations of active site-directed inhibitors when targeting a multifunctional protease.

AUTHOR CONTRIBUTION

Vidhu Sharma designed and performed experiments and wrote the paper; Anthony O'Donoghue performed and analysed subsite profiling experiments; Preety Panwar performed the collagen degradation experiment with DHT, the determination of the inhibitor potency of DHT towards CatV and CatS, and appropriate binding assays in the presence of DHT; Rafael Guido performed molecular docking of DHT on CatK; Haoran Cui determined IC_{50} of DHT for collagen degradation by CatK; Charles Craik reviewed the paper before submission; Dieter Brömme designed experiments and wrote the paper.

ACKNOWLEDGEMENTS

Gethin Owen is acknowledged for his help with SEM sample preparation. Raymond Pan is acknowledged for his help with WT CatK purification. We thank Ingrid Ellis for her editorial assistance in the final preparation of the paper.

FUNDING

The present work was supported by the Canadian Institutes of Health Research [grant numbers MOP-89974 and MOP-125866] and the Natural Sciences & Engineering Research Council of Canada [grant number RGPIN-326803-13 (to D.B.)] and the National Institutes of Health [grant number R01-CA128765] and a Department of Defence Idea Award [number PC111318 (to C.S.C.)].

REFERENCES

- 1 Yasuda, Y., Li, Z., Greenbaum, D., Bogyo, M., Weber, E. and Brömme, D. (2004) Cathepsin V, a novel and potent elastolytic activity expressed in activated macrophages. J. Biol. Chem. 279, 36761–36770 CrossRef PubMed
- 2 Brömme, D. (2011) Cystein cathepsins and the skeleton. Clin. Rev. Bone Miner. Metab. 9, 83–93 CrossRef
- Fonovic, M. and Turk, B. (2014) Cysteine cathepsins and extracellular matrix degradation. Biochim. Biophys. Acta 1840, 2560–2570 CrossRef PubMed
- 4 Kiviranta, R., Morko, J., Uusitalo, H., Aro, H. T., Vuorio, E. and Rantakokko, J. (2001) Accelerated turnover of metaphyseal trabecular bone in mice overexpressing cathepsin K. J. Bone Miner. Res. 16, 1444–1452 <u>CrossRef PubMed</u>
- Yasuda, Y., Kaleta, J. and Brömme, D. (2005) The role of cathepsins in osteoporosis and arthritis: rationale for the design of new therapeutics. Adv. Drug Deliv. Rev. 57, 973–993 CrossRef PubMed
- 6 Lutgens, S. P., Cleutjens, K. B., Daemen, M. J. and Heeneman, S. (2007) Cathepsin cysteine proteases in cardiovascular disease. FASEB J. 21, 3029–3041 CrossRef PubMed
- 7 Sukhova, G. K. and Shi, G. P. (2006) Do cathepsins play a role in abdominal aortic aneurysm pathogenesis? Ann. N. Y. Acad. Sci. 1085, 161–169 CrossRef
- 8 Brömme, D. and Lecaille, F. (2009) Cathepsin K inhibitors for osteoporosis and potential off-target effects. Expert Opin. Investig. Drugs 18, 585–600 CrossRef PubMed
- 9 Brömme, D., Okamoto, K., Wang, B. B. and Biroc, S. (1996) Human cathepsin O2, a matrix protein-degrading cysteine protease expressed in osteoclasts. Functional expression of human cathepsin O2 in *Spodoptera frugiperda* and characterization of the enzyme. J. Biol. Chem. 271, 2126–2132 CrossRef PubMed
- 10 Bossard, M. J., Tomaszek, T. T., Thompson, S. K., Amegadzies, B. Y., Hannings, C. R., Jones, C., Kurdyla, J. T., McNulty, D. E., Drake, F. H., Gowen, M. and Levy, M. A. (1996) Proteolytic activity of human osteoclast cathepsin K. Expression, purification, activation, and substrate identification. J. Biol. Chem. 271, 12517–12524 CrossRef PubMed
- 11 Samokhin, A. O., Wong, A., Saftig, P. and Brömme, D. (2008) Role of cathepsin K in structural changes in brachiocephalic artery during progression of atherosclerosis in apoE-deficient mice. Atherosclerosis 200, 58–68 CrossRef PubMed
- 12 Podgorski, I. (2009) Future of anticathepsin K drugs: dual therapy for skeletal disease and atherosclerosis? Future Med. Chem. 1, 21–34 PubMed
- 13 Chapurlat, R. D. (2014) Odanacatib for the treatment of postmenopausal osteoporosis. Expert Opin. Pharmacother. 15, 97–102 CrossRef PubMed
- 14 Tepel, C., Brömme, D., Herzog, V. and Brix, K. (2000) Cathepsin K in thyroid epithelial cells: sequence, localization and possible function in extracellular proteolysis of thyroglobulin. J. Cell Sci. 113, 4487–4498 PubMed
- 15 Zhang, D., Leung, N., Weber, E., Saftig, P. and Brömme, D. (2011) The effect of cathepsin K deficiency on airway development and TGF-β₁ degradation. Respir. Res. 12, 72 CrossRef PubMed
- 16 Godat, E., Lecaille, F., Desmazes, C., Duchene, S., Weidauer, E., Saftig, P., Brömme, D., Vandier, C. and Lalmanach, G. (2004) Cathepsin K: a cysteine protease with unique kinin-degrading properties. Biochem. J. 383, 501–506 CrossRef PubMed
- 17 Lendeckel, U., Kahne, T., Ten Have, S., Bukowska, A., Wolke, C., Bogerts, B., Keilhoff, G. and Bernstein, H. G. (2009) Cathepsin K generates enkephalin from beta-endorphin: a new mechanism with possible relevance for schizophrenia. Neurochem. Int. 54, 410–417 CrossRef PubMed
- 18 Buhling, F., Rocken, C., Brasch, F., Hartig, R., Yasuda, Y., Saftig, P., Brömme, D. and Welte, T. (2004) Pivotal role of cathepsin K in lung fibrosis. Am. J. Pathol. 164, 2203–2216 CrossRef PubMed
- 19 Dauth, S., Sirbulescu, R. F., Jordans, S., Rehders, M., Avena, L., Oswald, J., Lerchl, A., Saftig, P. and Brix, K. (2011) Cathepsin K deficiency in mice induces structural and metabolic changes in the central nervous system that are associated with learning and memory deficits. BMC Neurosci. 12, 74 CrossRef PubMed
- 20 Rajan, N., Habermehl, J., Cote, M. F., Doillon, C. J. and Mantovani, D. (2006) Preparation of ready-to-use, storable and reconstituted type I collagen from rat tail tendon for tissue engineering applications. Nat. Protoc. 1, 2753–2758 CrossRef PubMed
- 21 Friesner, R. A., Banks, J. L., Murphy, R. B., Halgren, T. A., Klicic, J. J., Mainz, D. T., Repasky, M. P., Knoll, E. H., Shelley, M., Perry, J. K. et al. (2004) Glide: a new approach for rapid, accurate docking and scoring. 1. Method and assessment of docking accuracy. J. Med. Chem. 47, 1739–1749 CrossRef PubMed

- 22 Halgren, T. A., Murphy, R. B., Friesner, R. A., Beard, H. S., Frye, L. L., Pollard, W. T. and Banks, J. L. (2004) Glide: a new approach for rapid, accurate docking and scoring. 2. Enrichment factors in database screening. J. Med. Chem. 47, 1750–1759 CrossRef PubMed
- 23 Dossetter, A. G., Beeley, H., Bowyer, J., Cook, C. R., Crawford, J. J., Finlayson, J. E., Heron, N. M., Heyes, C., Highton, A. J., Hudson, J. A. et al. (2012) (1R,2R)-N-(1-cyanocyclopropyl)-2-(6-methoxy-1,3,4,5-tetrahydropyrido[4,3-b]indole -2-carbonyl)cyclohexanecarboxamide (AZD4996): a potent and highly selective cathepsin K inhibitor for the treatment of osteoarthritis. J. Med. Chem. 55, 6363–6374 CrossRef PubMed
- Friesner, R. A., Murphy, R. B., Repasky, M. P., Frye, L. L., Greenwood, J. R., Halgren, T. A., Sanschagrin, P. C. and Mainz, D. T. (2006) Extra precision glide: docking and scoring incorporating a model of hydrophobic enclosure for protein-ligand complexes. J. Med. Chem. 49, 6177–6196 CrossRef PubMed
- 25 Du, X., Chen, N. L., Wong, A., Craik, C. S. and Brömme, D. (2013) Elastin degradation by cathepsin V requires two exosites. J. Biol. Chem. 288, 34871–34881 CrossRef PubMed
- 26 Panwar, P., Du, X., Sharma, V., Lamour, G., Castro, M., Li, H. and Brömme, D. (2013) Effects of cysteine proteases on the structural and mechanical properties of collagen fibers. J. Biol. Chem. 288, 5940–5950 CrossRef PubMed
- 27 Hou, W. S., Li, Z., Buttner, F. H., Bartnik, E. and Brömme, D. (2003) Cleavage site specificity of cathepsin K toward cartilage proteoglycans and protease complex formation. Biol. Chem. 384, 891–897 CrossRef PubMed
- 28 Novinec, M., Grass, R. N., Stark, W. J., Turk, V., Baici, A. and Lenarcic, B. (2007) Interaction between human cathepsins K, L, and S and elastins: mechanism of elastinolysis and inhibition by macromolecular inhibitors. J. Biol. Chem. 282, 7893–7902 CrossRef PubMed
- 29 Bhaskaran, R., Palmier, M. O., Lauer-Fields, J. L., Fields, G. B. and Van Doren, S. R. (2008) MMP-12 catalytic domain recognizes triple helical peptide models of collagen V with exosites and high activity. J. Biol. Chem. 283, 21779–21788 CrossRef PubMed
- 30 Fulcher, Y. G. and Van Doren, S. R. (2011) Remote exosites of the catalytic domain of matrix metalloproteinase-12 enhance elastin degradation. Biochemistry 50, 9488–9499 CrossRef PubMed
- 31 Li, Z., Hou, W. S., Escalante-Torres, C. R., Gelb, B. D. and Brömme, D. (2002) Collagenase activity of cathepsin K depends on complex formation with chondroitin sulfate. J. Biol. Chem. 277, 28669–28676 CrossRef PubMed
- 32 Li, Z., Kienetz, M., Cherney, M. M., James, M. N. and Brömme, D. (2008) The crystal and molecular structures of a cathepsin K:chondroitin sulfate complex. J. Mol. Biol. 383, 78–91 CrossRef PubMed
- 33 Cherney, M. M., Lecaille, F., Kienitz, M., Nallaseth, F. S., Li, Z., James, M. N. and Brömme, D. (2011) Structure-activity analysis of cathepsin K/chondroitin 4-sulfate interactions. J. Biol. Chem. 286, 8988–8998 CrossRef PubMed
- 34 Gelb, B. D., Brömme, D. and Desnick, R. J. (2001) Pycnodysostosis: cathepsin K deficiency. In The Metabolic and Molecular Bases of Inherited Diseases (Sriver, C. R., Beaudet, A. L., Valle, D. and Sly, W. C. S., eds), vol. III, part 16, pp. 3453–3468, McGraw-Hill
- 35 Hou, W.-S., Brömme, D., Zhao, Y., Mehler, E., Dushey, C., Weinstein, H., Miranda, C. S., Fraga, C., Greig, F., Carey, J. et al. (1999) Cathepsin K: characterization of novel mutations in the pro and mature polypeptide regions causing pycnodysostosis. J. Clin. Invest. 103, 731–738 CrossRef PubMed
- 36 Overall, C. M. (2001) Matrix metalloproteinase substrate binding domains, modules and exosites. Overview and experimental strategies. Methods Mol. Biol. 151, 79–120 <u>PubMed</u>
- 37 Bertini, I., Fragai, M., Luchinat, C., Melikian, M., Toccafondi, M., Lauer, J. L. and Fields, G. B. (2012) Structural basis for matrix metalloproteinase 1-catalyzed collagenolysis. J. Am. Chem. Soc. 134, 2100–2110 <u>CrossRef PubMed</u>
- Manka, S. W., Carafoli, F., Visse, R., Bihan, D., Raynal, N., Farndale, R. W., Murphy, G., Enghild, J. J., Hohenester, E. and Nagase, H. (2012) Structural insights into triple-helical collagen cleavage by matrix metalloproteinase 1. Proc. Natl. Acad. Sci. U.S.A. 109, 12461–12466 CrossRef PubMed
- 39 Fields, G. B. (2013) Interstitial collagen catabolism. J. Biol. Chem. 288, 8785–8793 CrossRef PubMed
- 40 Stura, E. A., Visse, R., Cuniasse, P., Dive, V. and Nagase, H. (2013) Crystal structure of full-length human collagenase 3 (MMP-13) with peptides in the active site defines exosites in the catalytic domain. FASEB J. 27, 4395–4405 CrossRef PubMed
- 41 Lecaille, F., Choe, Y., Brandt, W., Li, Z., Craik, C. S. and Bromme, D. (2002) Selective inhibition of the collagenolytic activity of human cathepsin K by altering its S2 subsite specificity. Biochemistry 41, 8447–8454 <u>CrossRef PubMed</u>

- 42 Bannwarth, L., Goldberg, A. B., Chen, C. and Turk, B. E. (2012) Identification of exosite-targeting inhibitors of anthrax lethal factor by high-throughput screening. Chem. Biol. 19, 875–882 CrossRef PubMed
- 43 Wang, W., Liu, Y. and Lazarus, R. A. (2013) Allosteric inhibition of BACE1 by an exosite-binding antibody. Curr. Opin. Struct .Biol. 23, 797–805 CrossRef PubMed
- 44 Costa, A. G., Cusano, N. E., Silva, B. C., Cremers, S. and Bilezikian, J. P. (2011) Cathepsin K: its skeletal actions and role as a therapeutic target in osteoporosis. Nat. Rev. Rheumatol. 7, 447–456 CrossRef PubMed
- 45 Cui, L., Wu, T., Liu, Y. Y., Deng, Y. F., Al, C. M. and Chen, H. Q. (2004) Tanshinone prevents cancellous bone loss induced by ovariectomy in rats. Acta Pharmacol. Sin. 25, 678–684 PubMed
- 46 Kim, H. H., Kim, J. H., Kwak, H. B., Huang, H., Han, S. H., Ha, H., Lee, S. W., Woo, E. R. and Lee, Z. H. (2004) Inhibition of osteoclast differentiation and bone resorption by tanshinone IIA isolated from *Salvia miltiorrhiza* Bunge. Biochem. Pharmacol. 67, 1647–1656 CrossRef PubMed

Received 16 July 2014/22 September 2014; accepted 3 October 2014 Published as BJ Immediate Publication 3 October 2014, doi:10.1042/BJ20140809

- 47 Kim, H. K., Woo, E. R., Lee, H. W., Park, H. R., Kim, H. N., Jung, Y. K., Choi, J. Y., Chae, S. W., Kim, H. R. and Chae, H. J. (2008) The correlation of *Salvia miltiorrhiza* extract-induced regulation of osteoclastogenesis with the amount of components tanshinone I, tanshinone IIA, cryptotanshinone, and dihydrotanshinone. Immunopharmacol. Immunotoxicol. 30, 347–364 CrossRef PubMed
- 48 Xu, S., Little, P. J., Lan, T., Huang, Y., Le, K., Wu, X., Shen, X., Huang, H., Cai, Y., Tang, F., Wang, H. and Liu, P. (2011) Tanshinone II-A attenuates and stabilizes atherosclerotic plaques in apolipoprotein-E knockout mice fed a high cholesterol diet. Arch. Biochem. Biophys. 515, 72–79 CrossRef PubMed
- 49 Guo, Y., Li, Y., Xue, L., Severino, R. P., Gao, S., Niu, J., Qin, L. P., Zhang, D. and Brömme, D. (2014) Salvia miltiorrhiza: An ancient Chinese herbal medicine as a source for anti-osteoporotic drugs. J. Ethnopharmacol. 155, 1401–1416 CrossRef PubMed
- 50 Novinec, M., Korenc, M., Caflisch, A., Ranganathan, R., Lenarcic, B. and Baici, A. (2014) A novel allosteric mechanism in the cysteine peptidase cathepsin K discovered by computational methods. Nat. Commun. 5, 3287 CrossRef PubMed